CHAPTER V

APPARATUS AND PROCEDURE

The original Taylor dispersion apparatus constructed at Texas A&M has been described in detail by Matthews and Akgerman (1987a) and Matthews (1986). In this chapter, the design and operation of the original apparatus are reviewed. Specific modifications to the original apparatus and procedure are then discussed. The chapter concludes with a detailed description of the solutes and solvents which were selected for this study and a summary of the specific experimental conditions which were investigated during this research.

A. ORIGINAL APPARATUS AND PROCEDURE

The original apparatus shown is shown in Figure 5.1 and was operated as follows. The solvent was maintained at room temperature in a reservior where it is continuously sparged with helium. From the reservior, the solvent was pumped by a chromatographic pump through a 4 meter section of pre-heat tubing contained within a heated enclosure. The pure solvent then left the enclosure to flow through the reference side of a refractive index detector. The temperature of the refractive index detector was maintained at a constant temperature slightly above ambient by circulating constant temperature water through a jacket within the detector. Following the refractive index detector, the pure solvent flowed back into the heated enclosure and then passed through a chromatographic injection valve contained within the enclosure.

The solute solution to be injected was normally 8 mole percent of liquid solute dissolved in solvent or solvent saturated with the solute gas. The solute solution was prepared external to the heated enclosure and then pumped through the solute side

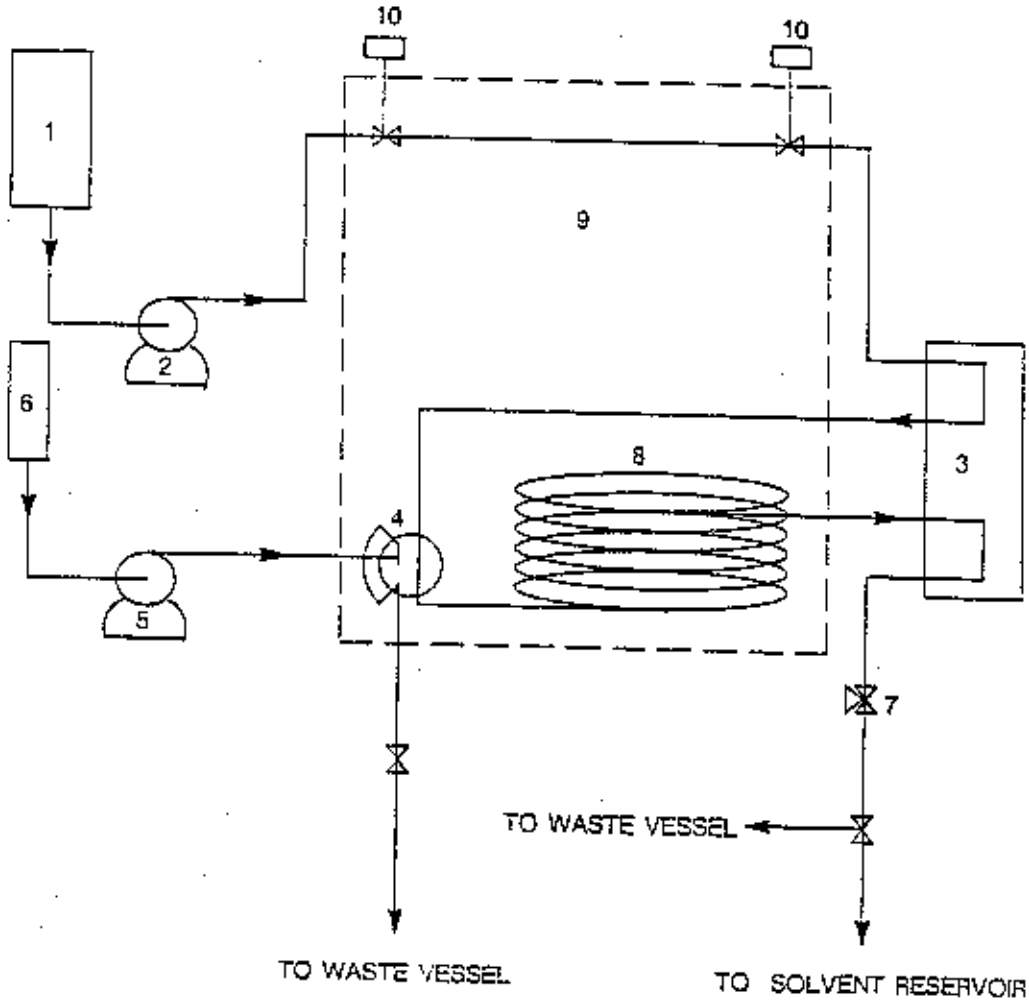

1. Solvent reservoir
2. Solvent pump
3. Refractive index detector
4. 6-port sample injection valve
5. Sample injection pump
6. Sample solution
7. Backpressure regulator
8. Coiled dispersion tube
9. Heated enclosure
10. Pressure transducers

Figure 5.1. Schematic diagram of original Taylor dispersion apparatus.

of the injection valve to load the valve. Pressure on the solute loop was maintained at approximately the same pressure as that of the flowing solvent stream using an adjustable check valve.

Following injection, the solute pulse was carried by the solvent stream through 43.55 meters of coiled 0.001 m I.D. stainless steel tubing before exiting the enclosure. The diffusion tube was coiled on an aluminum ring (0.16 m radius) that fit snugly inside the enclosure. Void space inside the enclosure was filled with aluminum shot so that the system was thermally massive. A microcomputer was used to monitor and control the temperature of the enclosure to within 0.5 K of the desired temperature during the course of an experiment. Reported temperatures were actually the average of temperatures recorded from four separate thermistors which had been calibrated with a standard platinum resistance thermometer. The same microcomputer was also used to monitor two calibrated strain gauge pressure transducers. Matthews (1986) reported that the pressure for each experiment was accurate to within better than 1 psi. The configuration of the data acquisition system is shown in Figure 5.2.

Upon leaving the heated enclosure, approximately two to three hours following injection, the solute pulse, which had spread into a Gaussian shaped peak, was carried through a short length of connecting tubing into the sample side of the refractive index detector. The detector output voltage was recorded by a second microcomputer every five seconds. For each eluting dispersion peak, these recorded data were then used to determine D_{12}^{o} using the moment method which was explained previously.

From the detector, the stream flowed through a backpressure regulator which maintained a constant pre-set pressure in the diffusion coil. The liquid solvent

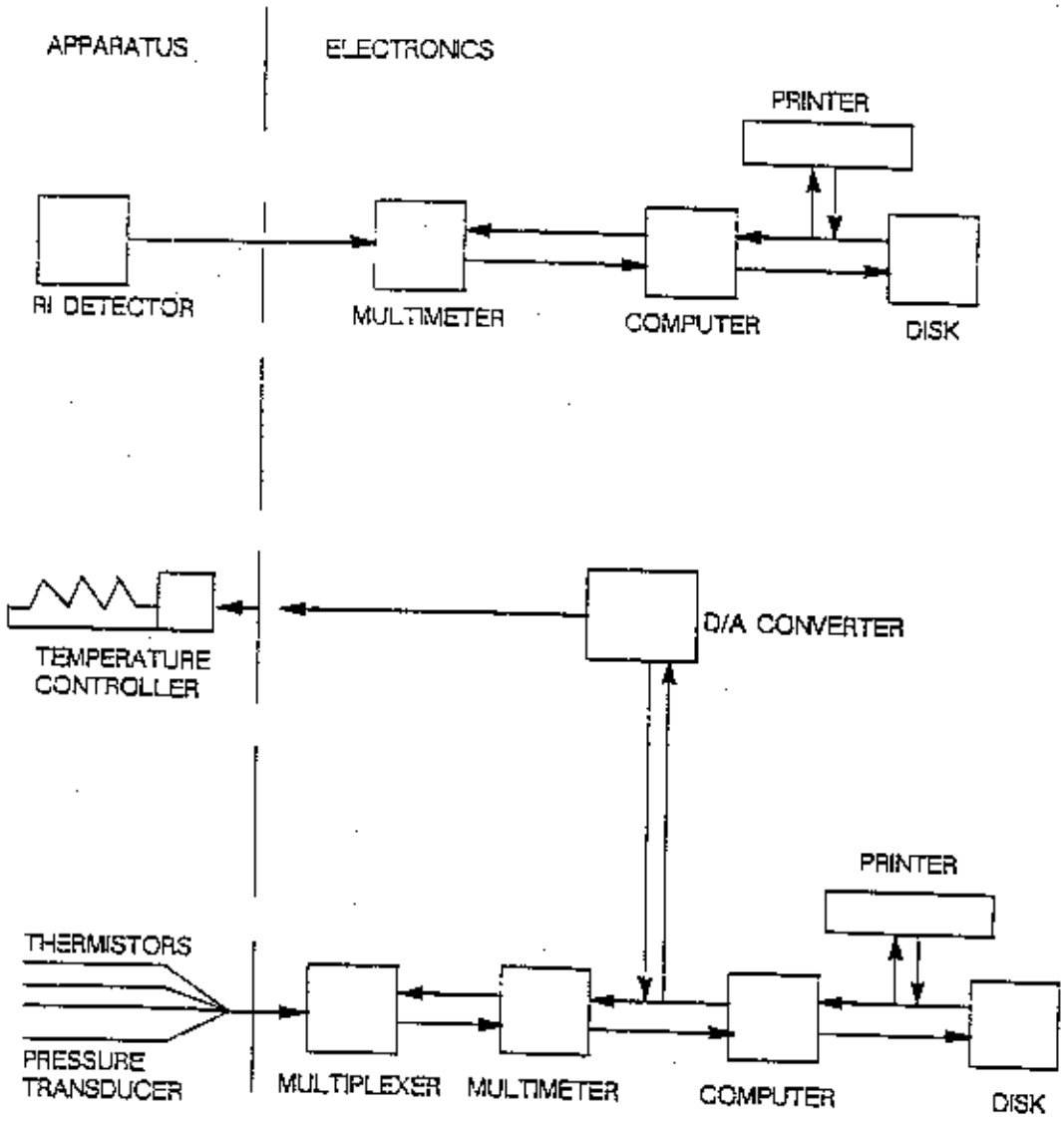

Figure 3.2. Schematic diagram of data acquisition and control system.

was either wasted or recycled back to the solvent reservoir by means of a 3-way valve. Solvent mass flow rates, required for solvent density calculations, were easily measured by collecting and weighing the wasted solvent stream over a measured time interval.

B. POTENTIAL SOURCES OF ERROR

The original apparatus was constructed and operated in accordance with the design criteria of Alizadeh et al. (1980). These criteria ensure that potential errors due to anomalies between the actual apparatus and the theory can be ignored. Matthews (1986) demonstrated that the original apparatus was constructed and operated so that resulting systematic errors in the diffusion coefficients due to the following anomolies were negligible (less than 0.5% total); the finite volume of the injection pulse; the finite length of the connecting tubing to the detector; the finite volume of the detector cell; the nonuniformity of the diffusion tube cross section; and the coiling of the diffusion tube. Matthews (1986) also demonstrated that the voltage response of the refractive index detector was proportional to concentration as expected.

Of the potential sources of error, the coiling of the diffusion tube is of greatest concern in a practical apparatus. The coiling of the tube creates secondary flows which are not accounted for in any of the mathematical models for Taylor dispersion, and thus results in potentially erroneous values for the calculated diffusion coefficient. Since any analysis of the secondary flow effects due to coiling is inherently associated with the choice of the mathematical model for Taylor dispersion, this source of error will be discussed further in Chapter VI. It will be shown that the choice of solvent flow rate is critical.

Table 5.1 Specifications of Taylor Dispersion Apparatus

Description	Value ± Uncertainty
Length of Dispersion Tube (m)	43.55 ± 0.05
Radius of Diffusion Tube (m)	0.000523 ± 0.000002
Length of Connecting Tube (m)	0.52 ± 0.01
Radius of Connecting Tube (m)	0.000127 ± 0.000005
Radius of Diffusion Tube Coil (m)	0.157 ± 0.008
Volume of Detector Cell (μ l)	9

Chapter VI also includes an analysis of potential errors due to the uncertainty of the diffusion tube radius and length measurements. These measurements and other important dimensions of the apparatus are given in Table 5.1. The radius was originally determined by weighing sections of tubing from the same lot as the diffusion tube which were filled with distilled deionized water. The radius was calculated as;

$$r = \sqrt{\frac{m}{\pi \rho l}} \tag{5.1}$$

where m and ρ are the mass and density of the water in the tube, and l is the length of the tube section. The original uncertainty estimate for the radius reported by Matthews (1986) was only a rough approximation. Since the uncertainty of the radius will later by shown to have a significant effect on the uncertainty of the reported diffusion coefficients, the radius uncertainty was recalculated using a more formal analysis of errors. Using the following formula, with reasonable estimates of the maximum individual errors in measurement (Δm, Δl, and $\Delta \rho$), the maximum uncertainty in r was calculated.

$$\Delta r = \left|\frac{\partial r}{\partial m}\Delta m\right| + \left|\frac{\partial r}{\partial l}\Delta l\right| + \left|\frac{\partial r}{\partial \rho}\Delta \rho\right| \tag{5.2}$$

The maximum uncertainty in r was calculated to be no greater than $\pm 2 \times 10^{-6}$ m, as reported in Table 5.1.

C. DENSITY FROM TAYLOR DISPERSION

Density is an important parameter occurring in most correlations for the diffusion coefficient. Often density does not appear in these correlations directly, but is disguised as molar volume, the quotient of molecular weight and density.

Matthews and Akgerman (1987c) reported a technique which was used to accurately determine solvent density using the Taylor dispersion apparatus. The technique is based on the fact that solvent density is related to the Taylor dispersion peak retention time and solvent mass flow rate. First, a calibration experiment was performed with water (a solvent of known density). Then using the mass flow rate and peak retention time from this calibration experiment (superscipt (1)), densities of n-heptane, n-dodecane, and n-hexadecane were determined at various other conditions (superscript (2)) from;

$$\rho_2 = \rho_1 \frac{\dot{m}^{(2)}}{\dot{m}^{(1)}} \frac{\bar{t}^{(2)}}{\bar{t}^{(1)}} \frac{V_t^{(1)}}{V_t^{(2)}} \tag{5.3}$$

where the characteristic retention time is given by;

$$\bar{t} = L/\bar{u} \tag{5.4}$$

The ratio of the tube volume at the calibration temperature to the volume at the experimental temperature was easily calculated using the thermal expansion coefficient for stainless steel which is the tube material. The actual tube volume did not need to be calculated. Matthews and Akgerman (1987c) estimated the accuracy of the densities measured using the new technique to be 0.1%. Actual experiments indicated that the technique was actually slightly more accurate than this estimate.

D. MODIFICATIONS TO THE ORIGINAL APPARATUS

The original apparatus was extensively modified before data was collected using the solvents n-eicosane, n-octacosane, and Union Carbide FT wax, all of which are waxy solids at room temperature. All wetted parts of the apparatus needed to be maintained safely above the melting point of the circulating solvent. The limiting solvent was Fischer-Tropsch wax which melted at approximately 100°C. In order to safely meet this criteria, all modifications were designed to withstand at least 130°C. The following modifications were necessary;

1. All external lines, valves, and backpressure regulators were heat traced with electrical heating tape. Most external lines were physically rerouted for safety and convenience. Valves were remounted on a panel. It was also necessary to change some valve packings and all seals to withstand the elevated temperatures. All valves were disassembled and cleaned in an ultrasonic bath following the discovery that an internal thread lubricant in some of the valves was soluble in molten n-eicosane.

2. The chromatographic pump (LDC/Milton Roy Constametric) piston seals were replaced with high temperature seals obtained from the manufacturer. The hydraulic section of the pump was heat traced with electrical heating tapes. Provisions were made for separating the heated hydraulic section of the pump from the pump electronics, but these provisions did not prove to be necessary. Through careful control and maintenance, the pump was successfully operated at 130°C, which was far beyond the maximum operating temperature of 70°C suggested by the manufacturer.

3. The optical section of the detector was separated from the electronics of the detector. The optical portion of the refractive index detector (LDC/Milton Roy Refractomonitor III) which contains the wetted cell was removed from its housing and mounted in a custom made enclosure. This prevented damage to the sensitive electronics of the detector due to heat and/or accidental liquid leakage. The cell and entrance tubing was heated by circulating hot ethylene glycol through a jacket surrounding the cell assembly. The gasket separating the sample and reference sides of the cell was replaced with a custom high temperature gasket, (DuPont Kalrez^R, 10 mil thickness). These modifications produced the first differential refractive index meter capable of operating above 70°C. In fact, for the Fischer-Tropsch experiments, the detector cell was

operated continuously at 145°C for a period of approximately five days. It was necessary to operate the detector at this temperature with the FT wax in order to prevent a film from forming on the surface of the detector's prism.

4. A glass solvent feed tank with heating mantle and temperature controller was installed. A custom top with appropriate fittings was constructed.

5. All heated lines, valves, surfaces, etc. were well insulated. Electrical heating tapes were wired so that a single switch could be thrown to cut power to the tapes in case of emergency.

6. The sample delivery system was completely redesigned and then heated with electrical heating tapes. A detailed description of the new sample delivery system is given later in this chapter. The original sample delivery system, shown in Figure 5.1 used a check valve to control the pressure in the sample injection loop. This method of controlling pressure was highly inaccurate, making it very difficult to equalize sample loop pressure with the pressure in the diffusion tube prior to injection. The sample delivery system was redesigned so that nitrogen, supplied through a regulator from a high pressure cylinder could be used to apply pressure to the sample loop.

Figure 5.3 shows the redesigned sample delivery system as it was configured for delivery of liquid solutes. Pre-mixing liquid alkane solutes with molten solvents would have required an additional heated reservoir, and would have also required wasting large volumes of molten solvent to adequately flush the system between solutes. In order to avoid these difficulties, pure solute was pumped at room temperature into a heated tee where it was mixed with pure molten solvent pumped from the heated solvent feed tank. Both solute and solvent were pumped into the tee through narrow bore stainless steel capillary tubing. The capillary tubing provided high enough velocities at the entrance to the tee so that adequate mixing of flows was achieved. Pump flows were ratioed to deliver a 5-10 mole percent solute solution to the injection valve.

Referring to Figure 5.3, the procedure for injecting a liquid solute was as follows;

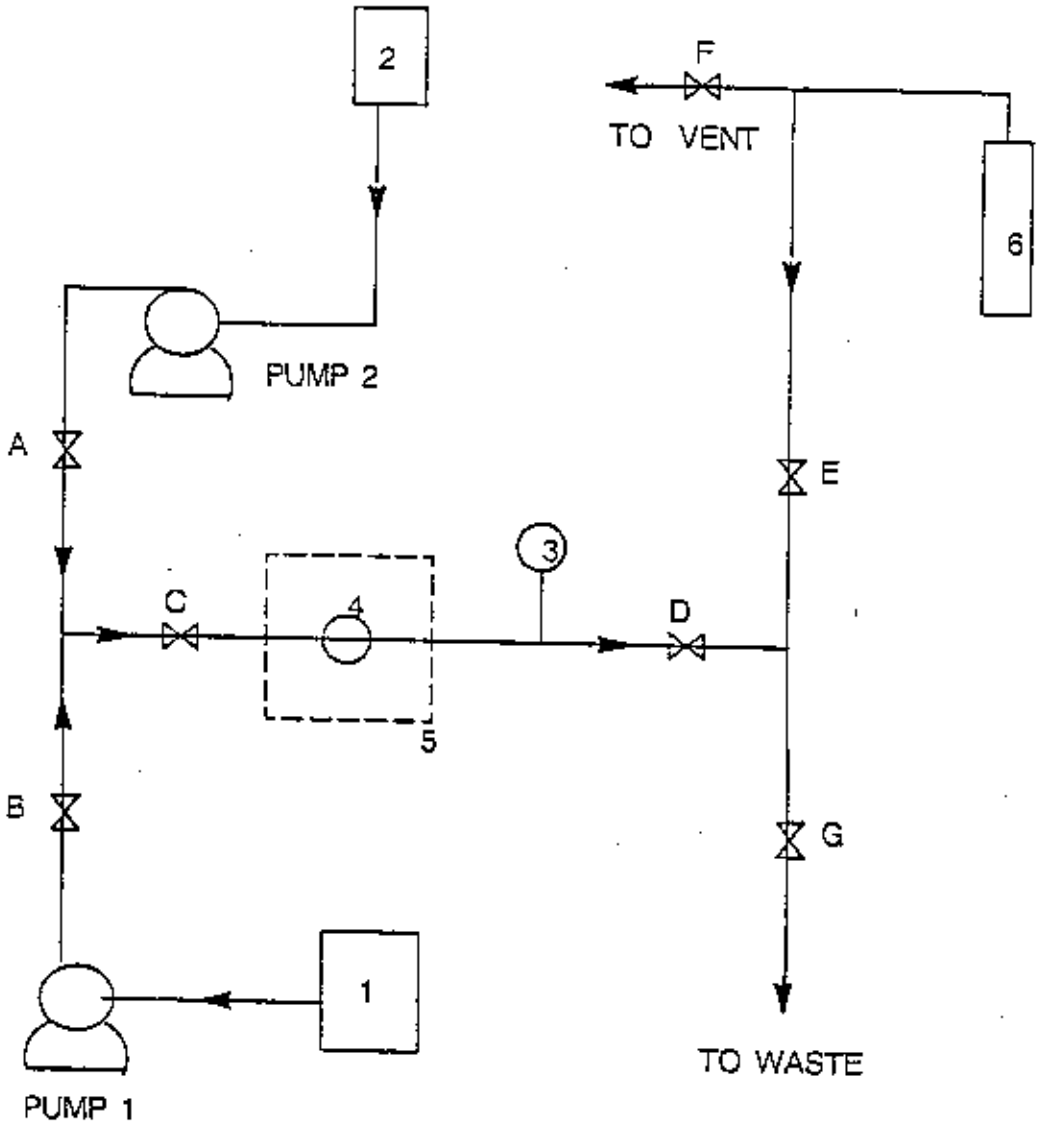

1. **Heated solvent feed reservoir**
2. **Pure solute reservoir (ambient conditions)**
3. **Pressure gauge**
4. **Sample injection valve**
5. **Boundary of heated enclosure**
6. **Regulated nitrogen cylinder**

Figure 5.3. Schematic of redesigned sample delivery system.

1. Valves B, E, and F were closed, all other valves opened. The injection valve was in the closed position.

2. Several volumes of the entire injection system were pumped through the system from the pure liquid solute reservoir.

3. Valve B was opened and pure molten solvent was pumped into the injection system. The flows of Pumps I and II were adjusted to pre-calibrated values to achieve a 5-10 mole % solution flowing through valve C, and at least two volumes of the solute-solvent mixture were pumped through the system.

4. Both Pumps I and II were turned off. Valves D, C, and G were closed in order. The nitrogen regulator was adjusted to 180 psia, approximately 20 psia less than the pressure in the diffusion tube. Valves E and D were slowly bled open, exposing the liquid in the sample loop to the pressure from the nitrogen. The nitrogen pressure was increased so that the sample loop pressure gauge shown in Figure 5.3 matched the diffusion tube pressure measured by the strain gauge pressure transducers (see Figure 5.1).

5. Valves D and E were closed. The injection valve was thrown open to expose the pure solvent flowing in the diffusion tube to the sample loop. (The injection valve was operated by a manually thrown electrical switch which activated a pneumatic drive.) The typical injection time was 10 seconds before the valve was closed. The approximate volume of each injection was 50 μl at the operating solvent flow rate.

6. Valves G and D were slowly opened releasing the sample loop pressure. Valve F was used to vent the nitrogen regulator.

7. Sufficient time was allowed between injections so that dispersion peaks would not overlap (usually at least 45 minutes between injections).

8. To inject the same solute again, valve C was opened. Pumps I and II were started at the same pre-determined flow rates. The solution was pumped through the system until a uniform liquid appeared at the exit from valve G. The procedure then resumed at Step 5.

9. To begin injections with a new solute, the entire procedure was repeated, starting with Step 1.

The experiments using gaseous solutes were originally conducted by injecting

samples of solvent which had been saturated under pressure with the gaseous solute. During the course of the experiments, several accidental injections of pure gas occured. Although the resulting dispersion peaks were much larger than the corresponding peaks for the saturated liquid injections, the calculated diffusion coefficients for the two types of injections agreed within experimental error. The phenomenon was investigated by injecting progressively larger amounts of each gaseous solute using n-octacosane as the solvent. This was accomplished by varying the injection time. Surprisingly, even full loop injections of gas, which lasted 12 seconds at the operating solvent flow rate, usually resulted in calculated diffusion coefficients which agreed with the results for the injections of the shortest possible duration (less than one-half second). Full loop injections corresponded to 100 μl of gas injected at the diffusion tube pressure of approximately 200 psia. By comparing relative peak heights, which are approximately proportional to the mass of the injection, the volume of the shortest possible duration injections was estimated to be approximately 20 μl. In order to minimize deviations from the ideal Taylor dispersion experiment, injections of the shortest possible duration were used to collect all subsequent gaseous solute data.

The injected volume of gas begins dissolving upon injection in the region of the diffusion tube where a mathematical solution to even simple Taylor dispersion has not yet been developed (see Chapter VI). Although the phenomenon cannot be described mathematically, it seems reasonable to conclude from the experimental results that a small bubble (or bubbles) enters the diffusion tube and dissolves quickly enough so that in practice the experiment is nearly identical to the experiment where a sample of gas-saturated solvent is injected. For this reason, the technique is referred to as the quick bubble method.

Table 5.2. Validation of Quick Bubble Injection Technique for Hydrogen in n-Octacosane at 180°C, 200 psia
($10^9 D^o_{12}$, m^2/sec)

Saturated Liquid Injection Method (5 replicates)	Quick Bubble Injection Method (3 replicates)
29.50	29.33
29.76	29.57
29.36	29.42
29.30	
29.35	
29.45 ± 0.19[1]	29.44 ± 0.12[1]

1. Average ± one standard deviation.

Table 5.2 illustrates the precision and accuracy of the quick bubble technique for hydrogen, the least soluble gas used in this study. Diffusion coefficients were calculated using the method presented in Chapter VI.

The data using the quick bubble technique was collected four calendar days following the saturated liquid data. On the interim days the apparatus was operated at various temperatures. Table 5.2 therefore illustrates not only the accuracy and precision of the quick bubble method, but also illustrates the capability of the apparatus to reproduce previous experimental conditions.

The quick bubble technique greatly simplified the experiment by eliminating the need for an external heated saturator and the associated heated tubes, valves, and pumps. The method also minimized the possibility of contaminated solute injections and permitted data to be collected without wasting large quantities of the solvents which were very expensive. Pure gaseous solutes were injected using the injection system shown in Figure 5.3 with only minor modifications. The procedure was as follows;

1. Valves A, E, and F were closed and all other valves opened. The injection system was then pumped clean with several volumes of pure solvent. Valve B was then closed.

2. The tubing from Pump II to valve A was disconnected at the valve. The heated injection system was blown dry with nitrogen.

3. The waste line from valve G was attached to a line which vented to a laboratory hood. (Steps 1 through 3 were only performed prior to the collection of all gaseous solute data for each solvent.)

4. The injection system was purged with the chosen solute gas (carbon dioxide, carbon monoxide, or hydrogen) through valve A.

5. Valve D was closed. Solute gas pressure was increased to match the pressure in the diffusion tube (typically 200 psia). Valve C was closed, isolating the sample loop.

6. The sample injection valve operating switch was opened and closed as quickly as possible (total injection time was less than one half second) in order to inject a small quantity of gas into the diffusion tube.

7. Sufficient time was allowed between injections so that dispersion peaks would not overlap (usually at least 30 minutes between gaseous solute injections).

8. To inject the same solute, the procedure was resumed at Step 4.

9. To inject a different gas solute, the regulator for the previous gas cylinder was vented to the hood through the injection system. Procedure then resumed at Step 4. NOTE: To eliminate the possibility of any reaction in the injection system, hydrogen and carbon monoxide were never injected back to back without first purging the system with nitrogen.

E. SPECIAL CONSIDERATIONS WITH MOLTEN SOLVENTS

The heated solvent feed tank was purged constantly with helium to remove dissolved air from the molten solvent. During the initial trial experiments using n-eicosane as the solvent, large spikes sporadically occured in the baseline output from the refractive index detector. These spikes were eventually traced to helium

bubbles which formed in the suction lines leading to the chromatographic pump feeding the diffusion tube. The bubbles lodged in the suction check valves of the pump, disrupting the constant pump flow which was required to maintain a steady baseline.

One possible solution to the problem was to pressurize the feed tank, but since the feed tank had not been designed as a pressure vessel, extensive changes would have been required. Since the solubility of helium increases with temperature in most organic solvents (Gerrard, 1980), an alternative solution was to maintain all suction lines at a higher temperature than the temperature at which the solvent was saturated in the feed tank. The problem was eventually eliminated by maintaining all wetted lines on the suction side of the solvent feed pump at a temperature at least 10°C higher than the solvent feed tank temperature. In order to achieve this temperature gradient without overheating the pump, the solvent feed tank was maintained at a temperature only slightly above the melting point of the solvent.

F. COMPOSITION OF SOLUTES AND SOLVENTS

Normal heptane, octane, hexadecane, eicosane, and octacosane were obtained from Alfa Chemicals. Normal dodecane was obtained from Phillips Petroleum. All purities were stated as at least 99 mol%. All bottled gases were used as received.

The sample of Fischer-Tropsch wax used in this study was generously donated by Union Carbide via Dr. G. Sturm of the National Institute for Petroleum and Energy Research (NIPER) Center. The sample had been originally sent to Dr. R.P. Anderson of NIPER on December 1, 1986. The sample was obtained from a Union Carbide pilot plant reactor using a proprietary cobalt catalyst and had been filtered through a 2 μl filter. A similar sample of Union Carbide FT wax was

analyzed by UOP (McArdle et al., 1986). For this whole wax sample, the carbon number was found to be 28. Only 0.45% of the carbons were branched, indicating a high percentage of n-paraffins.

A portion of the actual Fischer-Tropsch sample used in this study was analyzed by NIPER (Anderson, et al., 1987). Results for the whole wax sample are not yet available. However, an analysis of the heavy fraction containing only compounds with carbon numbers greater than C_{22} has been completed. This fraction was 80% alkanes and 7% olefins. The olefins were primarily mono-olefins.

From the available analyses of the Union Carbide Fischer-Tropsch waxes, it was estimated that the whole wax sample contained at least 75% paraffins of which most were n-paraffins. The average carbon number was approximately 28. These general characterizations will prove useful when discussing the diffusion coefficients measured in the Fischer-Tropsch wax.

The Union Carbide FT wax sample was a soft milky white solid, which could easily be stirred. Throughout the sample, clear liquid droplets could be observed. Upon heating, the sample began to melt at approximately 60°C, but was not a consistent uniform liquid until 110°C. Above 110°C, the liquid was clear, but had a yellowish tint. Upon cooling and freezing the yellow tint disappeared and the solid returned to its original white color. The wax was not heated to its boiling point, but UOP found the boiling point of a similar sample of Union Carbide wax to be 286°C.

When the FT wax sample was heated slowly, a clear phase formed below the predominant organic phase. This phase was analyzed by Karl Fischer titration and found to be at least 90% water. The sample was carefully distilled at 100°C under slight vacuum to remove the water. The recovered distillate represented 7%

of the total liquid volume of the wax, and was primarily an aqueous phase. It was absolutely necessary to remove this water phase in order to operate our apparatus.

G. EXPERIMENTAL CONDITIONS

Mutual diffusion coefficients at near infinite dilution were measured for the solutes hydrogen, carbon monoxide, carbon dioxide, n-octane, n-dodecane, and n-hexadecane, in the solvents n-eicosane, n-octacosane, and Union Carbide Fischer-Tropsch reactor wax.

Since previous measurements have indicated that diffusion in alkane solvents is a very weak function of pressure over the range 0-500 psi, (Matthews and Akgerman (1987a), all measurements for this study were made at 200 psi, which is a typical operating pressure of a Fischer-Tropsch reactor. For the solvents n-eicosane and n-octacosane, solvent density and diffusion coefficients for all solutes were measured at 100, 140, 180, 220, and 260°C. For the Fischer-Tropsch wax, data was collected at 200, 220, 240, and 260°C, in order to cover the normal range of Fischer-Tropsch reaction temperatures.

The final reported values for the diffusion coefficients were calculated using an improved mathematical model for Taylor dispersion which is developed in Chapter VI. Final results are reported in Chapter VII.

CHAPTER VI

TAYLOR DISPERSION MODEL

In order to avoid the inherent errors associated with the moment and graphical methods, a new analysis method was developed based on the analytical solution to the Taylor dispersion problem. In this chapter, the details of the model are presented and the model is validated.

A. MATHEMATICAL DESCRIPTION OF MODEL

Before describing the new analysis method, it is necessary to explain how concentration is measured in a practical apparatus. In all existing Taylor dispersion apparatuses, including our own, concentration is not measured directly. Instead, a detector at the end of the diffusion tube outputs a voltage which is proportional to the solute concentration. The linear response of the refractive index detector used in this study has been demonstrated previously by Matthews (1986). Theoretically, the detector output voltage should remain steady when a peak is not eluting, but in practice the output often drifts linearly with time. In practice, the output voltage of the detector is also not exactly zero when peaks are not eluting. This offset voltage is referred to as the baseline voltage. For a model to accurately represent the raw voltage versus time data, it must account for these effects.

The starting point for the model was Equation 2.5 , the solution to the Taylor dispersion problem for the case of an impulse injection;

$$C_a = \frac{M}{\pi a^2 (4\pi K t)^{1/2}} \cdot \exp\left(\frac{-(L-\overline{u}t)^2}{4Kt}\right) \tag{2.5}$$

Since the detector output voltage is proportional to solute concentration, a mathe-

matical model for voltage was written as;

$$V = \frac{B_1}{t^{1/2}} \cdot exp\left[\frac{-(L - B_4 t)^2}{B_2 t}\right] + B_3 + B_5 t \tag{6.1}$$

The B terms are free parameters which must be fit to the data. B_3 and B_5 account for baseline offset and drift. B_4 is the average solvent velocity of the laminar flow profile in the diffusion tube. B_2 is simply a factor of four times greater than the K, the Taylor dispersion coefficient.

Given K, Equation 2.4 can be rearranged and solved for D_{12} using the quadratic formula. The resulting expression for D_{12} is;

$$D_{12} = \frac{K}{2} - \left(\frac{K^2}{4} - \frac{(a\overline{u})^2}{48}\right)^{1/2} \tag{6.2}$$

which may be written in terms of the model parameters as;

$$D_{12} = \frac{B_2}{8} - \left(\frac{B_2^2}{64} - \frac{(aB_4)^2}{48}\right)^{1/2} \tag{6.3}$$

Equations 6.2 and 6.3 represent the negative root of the quadratic. Although the positive root of the quadratic also results in a positive value for D_{12}, only the negative root has physical meaning in a practical apparatus using liquid solvents (see Grushka and Kikta, 1974; and Giddings and Seager, 1962). Values of D_{12} calculated using the negative root agree closely with literature values for D_{12} obtained using other methods, while values of D_{12} calculated using the positive root are typically several orders of magnitude greater.

Once the equation was developed for calculating D_{12} from the model parameters, the only remaining hurdle was to determine the best fit parameters of Equation 6.1. These parameters were determined using the voltage and time data which was recorded concurrently by computer at regular intervals as the peaks eluted through

the detector. This raw data was used to determine the set of B's which minimized the following non-linear least squares function;

$$F = \sum_{i=1}^{n} [V_{measured}(i) - V_{Equation\ 6.1}(i)]^2 \tag{6.4}$$

The set of B's which minimized the function was determined by solving simultaneously for the zeroes of the five equations which result from taking the first partial derivatives of Equation 6.4 respect to each model parameter. These five equations were solved using the Newton-Raphson iterative technique, which also required the full set of second partial derivatives of Equation 6.4. Analytical expressions were determined for all first and second partial derivatives in order to negate the possibility of roundoff errors and to ensure convergence. These analytical expressions are imbedded within the FORTRAN computer program containing the full model which is given in Appendix A.

Reasonable initial guesses for the model parameters were crucial for convergence to be achieved. All of the initial guesses were generated internally within the computer program containing the model. Highly accurate guesses for B_1 and B_2 were determined by employing a search routine to find the peak voltage maximum and then applying simple algebraic relationships which exist between the model and the analytical solution. B_4 is simply the average solvent flow rate and was accurately estimated from the following equation;

$$B_4 = \overline{u} \approx L/t_{max} \tag{6.5}$$

where t_{max} is the time corresponding to the peak voltage maximum. Levenspiel and Smith (1957) discussed this assumption in detail.

Accurate estimates for baseline slope, B_3, and baseline drift B_5, were determined by linearly interpolating between the starting and ending points of the peak

which were supplied as input to the program. However, it was necessary to change the form of the model slightly so that the initial guesses led to convergence. The model was modified to the following form;

$$V = \frac{B_1}{t^{1/2}} \cdot \exp\left[\frac{-(L - B_4 t)^2}{B_2 t}\right] + B_3 + B_5\,(t - t(1)) \tag{6.6}$$

where $t(1)$ is the time corresponding to the peak starting voltage. This model has better convergence properties than Equation 6.1 since B_3 is now the baseline value at the peak start. In Equation 6.1, B_3 was the extrapolated baseline value at the injection time which was typically two to three hours prior to the time of peak elution.

The most difficult parameter to estimate apriori is B_2, which is proportional to K, the Taylor dispersion coefficient. In order to estimate K, an estimate of D_{12} is necessary, but estimating D_{12} is often extremely difficult since data is rarely collected for systems with known diffusion coefficients. This problem was circumvented by writing a FORTRAN algorithm to simulate the graphical method presented in Chapter II. By incorporating the "graphical method" into the computer model, initial guesses were generated for D_{12} (and hence B_2) which led to rapid convergence. The computerized algorithm for the "graphical" method eliminated the human error element normally associated with the method.

B. HANDLING OF RAW DATA

The code for the new Taylor dispersion data analysis method was written in FORTRAN for a Hewlett-Packard 9000 computer which belonged to the Chemical Engineering Department at Texas A&M. Since the raw peak data was originally collected on 5.25 inch floppy disks in Commodore B-128 format, it was necessary to

upload the data to the HP-9000 prior to analysis. At first, available software was used to transfer the data with a phone modem, but the data transfer rate of 300 baud was intolerable. Unfortunately, software was not available for transferring the data over a hard wire.

Software was eventually developed which allowed the data to be transferred from the Commodore to the HP error-free at 4800 baud over a hard wire. Using this software, it took only 10-15 minutes to transfer a typical floppy disk containing 12,000 pairs of recorded voltage vs. time data from a single day of experiments. Once uploaded to the HP9000 the data was analyzed and then stored on 3.50 inch floppy disks in HP format. The data could then be easily reanalyzed if necessary.

C. MODEL VALIDATION USING GENERATED DATA

The entire method for Taylor dispersion data analysis was incorporated into one user-friendly computer package (see Appendix A). The computer model was written in general so that any number of the five model parameters could be fixed at their initial values and so that any of the computer generated initial guesses could be overidden by the user. Surprisingly these features proved to be unnecessary. The only required user input were the injection time and the approximate time interval bounding the peak.

The model was validated using an artificial peak which was generated using Equation 6.6. The magnitude of the artificial peak parameters were chosen to be typical of an actual generic peak measured in this study. Voltages were generated at 5 second intervals to coincide with the normal sampling rate of an actual experiment. The results of the model validation are shown in Figure 6.1, in the form of the actual model output.

```
TAYMOD (Taylor Dispersion Peak Model)
Developed by: J.B. Rodden (Dec. 1987)

HP9000 data filename: artpeak

Solvent name: ANY SOLVENT

Peak description: THIS IS A GENERATED PEAK USED TO TEST THE MODEL

Temperature :  21.00 C
Temperature compensated diffusion tube length:  43.55 m
Temperature compensated diffusion tube radius:  .52300E-03 m

Injection time:   0: 0: 0 (    0. s)

Peak start time:  1:26:40 ( 5200. s) - inj. time =  1:26:40 ( 5200. s)
Peak end time:    2: 1:40 ( 7300. s) - inj. time =  2: 1:40 ( 7300. s)
Peak maximum at:  1:43:35 ( 6215. s) - inj. time =  1:43:35 ( 6215. s)

Peak start value:  .00000 v
Peak end value:    .00042 v
Peak max value:   -.00106 v

Peak width at half height:  595.0 s

Preliminary estimate of D12 (see Sun and Chen, 1985):   1.1096 E-09 m**2/s

The model is:
v(i)=B1/SQRT(t(i))*exp(-(L-B4*t(i))**2/(B2*t(i)))+B3+B5*(t(i)-t(1))

B1=pre-exp constant (v*s**0.5)          B5=baseline drift (v/s)
B2=4*K (m**2/s)                         K=D12+(a*u)**2/48/D12 (m**2/s)
B3=baseline voltage (v)                 a=diffusion tube radius (m)
B4=u; avg. fluid velocity (m/s)         L=diffusion tube length (m)

Drift included in model?  y

                    B1             B2             B3             B4             B5
Initial values:  -.99946E-01   .10087E-02   .92547E-06   .70072E-02   .19981E-06
Final iteration: -.10000E+00   .10000E-02   .10000E-05   .70000E-02   .20000E-06

Convergence criteria:  (1) epsilon = .10E-14;  (2) max # of iterations = 25

Model converged following  7 iterations.

No. of points :   421                          Average error  :  .249507538E-20 v
Sum of sq res :   .310543867E-33 v**2          Avg abs error  :  .367777531E-18 v
Avg sq error  :   .737633888E-36 v**2          Max abs error  :  .477048956E-17 v
Std err of est:   .860903487E-18 v             Avg observation: -.169369297E-03 v
r-squared     :  1.000000000                   Avg prediction : -.169369297E-03 v

D12 (final model result):   1.1169 E-09 m**2/s

Taylor-Hunt criteria: D12/(u*a)=.305E-03 ?>>? a/(4*L)=.300E-05

Retention time, (L/B4):  1:43:41 ( 6221.4 s)

D12 (top 95.0% of peak; 248 pts;  1:33:50 thru  1:54:25):   1.1169 E-09 m**2/s
D12 (top 90.0% of peak; 219 pts;  1:34:55 thru  1:53: 5):   1.1169 E-09 m**2/s
D12 (top 85.0% of peak; 199 pts;  1:35:40 thru  1:52:10):   1.1169 E-09 m**2/s
D12 (top 80.0% of peak; 182 pts;  1:36:20 thru  1:51:25):   1.1169 E-09 m**2/s
D12 (top 60.0% of peak; 139 pts;  1:38: 0 thru  1:49:30):   1.1169 E-09 m**2/s
D12 (top 40.0% of peak; 104 pts;  1:39:25 thru  1:48: 0):   1.1169 E-09 m**2/s
D12 (top 20.0% of peak;  69 pts;  1:40:50 thru  1:46:30):   1.1169 E-09 m**2/s
D12 (top 10.0% of peak;  48 pts;  1:41:40 thru  1:45:35):   1.1169 E-09 m**2/s
D12 (top  5.0% of peak;  34 pts;  1:42:15 thru  1:45: 0):   1.1169 E-09 m**2/s
```

Figure 6.1. Results of model validation using a computer generated peak.

Figure 6.1 verifies that the convergence criteria was met simultaneously for all five model parameters following only seven iterations. The convergence criteria was defined as;

$$\left|\frac{B_{j,i} - B_{j,i-1}}{B_{j,i}}\right| < \epsilon \tag{6.7}$$

where j is the index of the model parameter and i counts the total number of iterations. For the model validation case, ϵ was 1 x 10^{-15}. The ability of the model to meet this criteria indicated that the model was able to generate the actual parameters to within the limits of FORTRAN double precision. Other simple error statistics included in Figure 6.1 confirmed the extreme accuracy of the model.

The bottom portion of the output in Figure 6.1 illustrates another feature of the model. Even though it is recommended to include generous sections of baseline when the peak interval is input, the model has the capability of calculating the diffusion coefficient using any fraction of the peak. For example, when the top x% of a peak is specified (see bottom of Figure 6.1), only the data points where the peak voltage meets the following criteria are used in the analysis;

$$|V - V_{baseline}| > \left(1 - \frac{x}{100}\right) |V_{maximum} - V_{baseline}| \tag{6.8}$$

When only a fraction of the peak is used, the baseline voltage is defined in terms of the parameters B_3 and B_5 and remains fixed at the values determined using the full peak. As expected, even when only the upper two percent of the peak was used in the analysis, the same diffusion coefficient was calculated for the generated peak data.

D. MODEL VALIDATION USING EXPERIMENTAL DATA

Of over 600 individual experimental peaks which were analyzed to determine diffusion coefficients, the computer generated initial guesses led to convergence in

all cases but one. In no case did the model converge to unreasonable values of the parameters.

Three examples were chosen to demonstrate the performance of the model. Figure 6.2 illustrates the excellent agreement between measured voltage and voltage predicted by the model for the first example peak (carbon dioxide in n-eicosane). For this peak, voltage was measured every 5 seconds, but is plotted only every 30 seconds. The full computer output for Example 1 is given in Appendix B.1. This ouput includes a tabulated list of all measured voltages, predicted voltages, and residuals.

Figure 6.3 is a similar plot for a peak resulting from the injection of dilute n-dodecane (C_{12}), into the solvent n-eicosane at 222°C, the same temperature as the experiment illustrated by Figure 6.2. Although the peak maximum occurs at approximately the same time, the C_{12} peak is considerably wider than the CO_2 peak because the diffusion coefficient of C_{12} is considerably less than the diffusion coefficient of CO_2 at the same experimental conditions. The full computer output for this example is given in Appendix B.2.

The third and final example peak is plotted in Figure 6.4. Example 3 is for n-octane (C_8) in n-octacosane (C_{28}). The corresponding computer output is given in Appendix B.3. This example ilustrates that the model fits the data extremely well even when the peak height is very small. Figure 6.4 has been plotted on an expanded scale, but the total peak height of approximately 6mV is actually a factor of 15 times less than the peak height of the carbon dioxide peak shown in Figure 6.2. The noise in the tail is on the order of 0.05mV. Using the response factor of the detector (1×10^6mV/RIU) the observed noise was estimated to be 5×10^{-8} RIU (Refractive Index Units). Assuming the detectable limit to be twice the noise

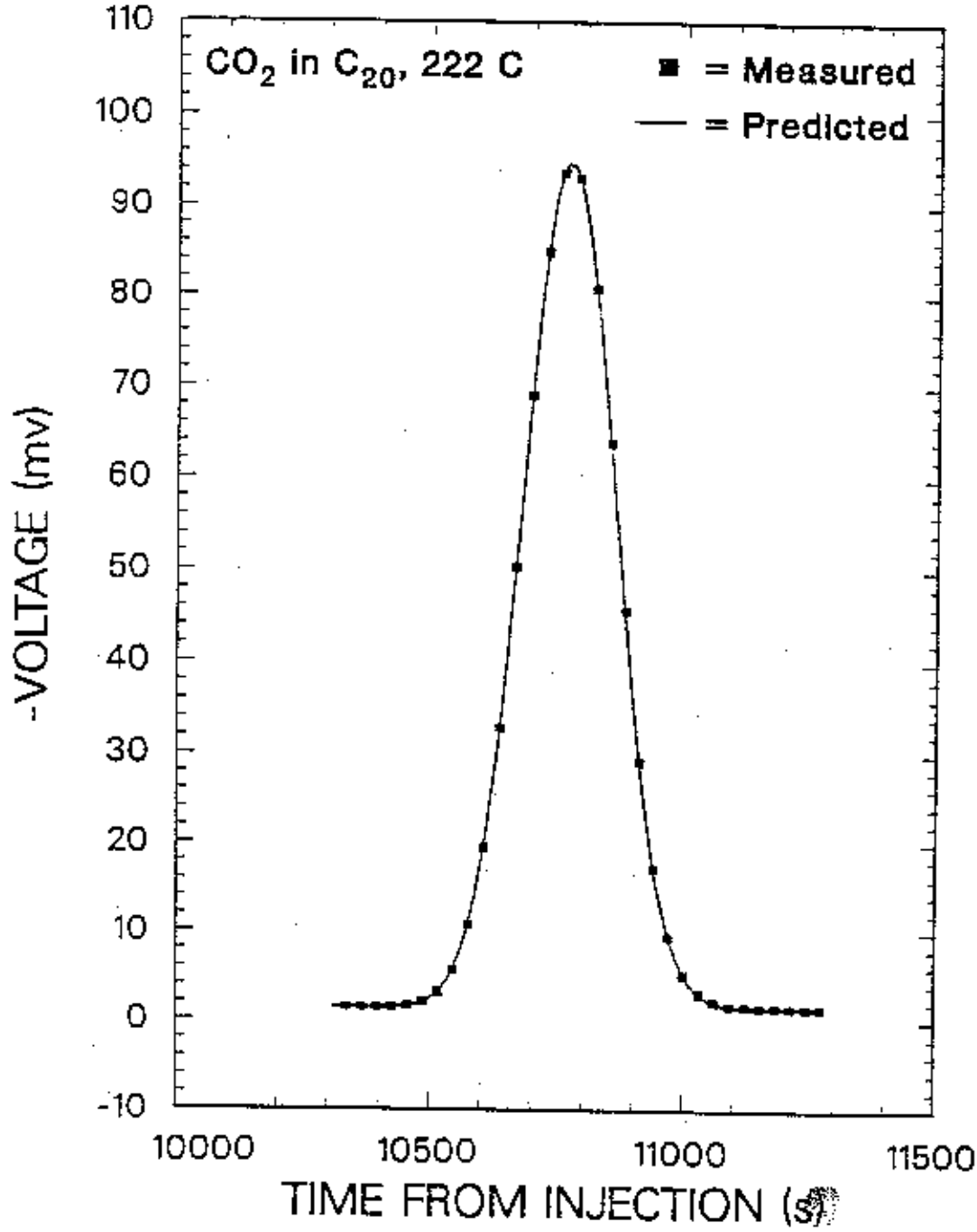

Figure 6.2. Model validation using a typical gaseous solute peak.

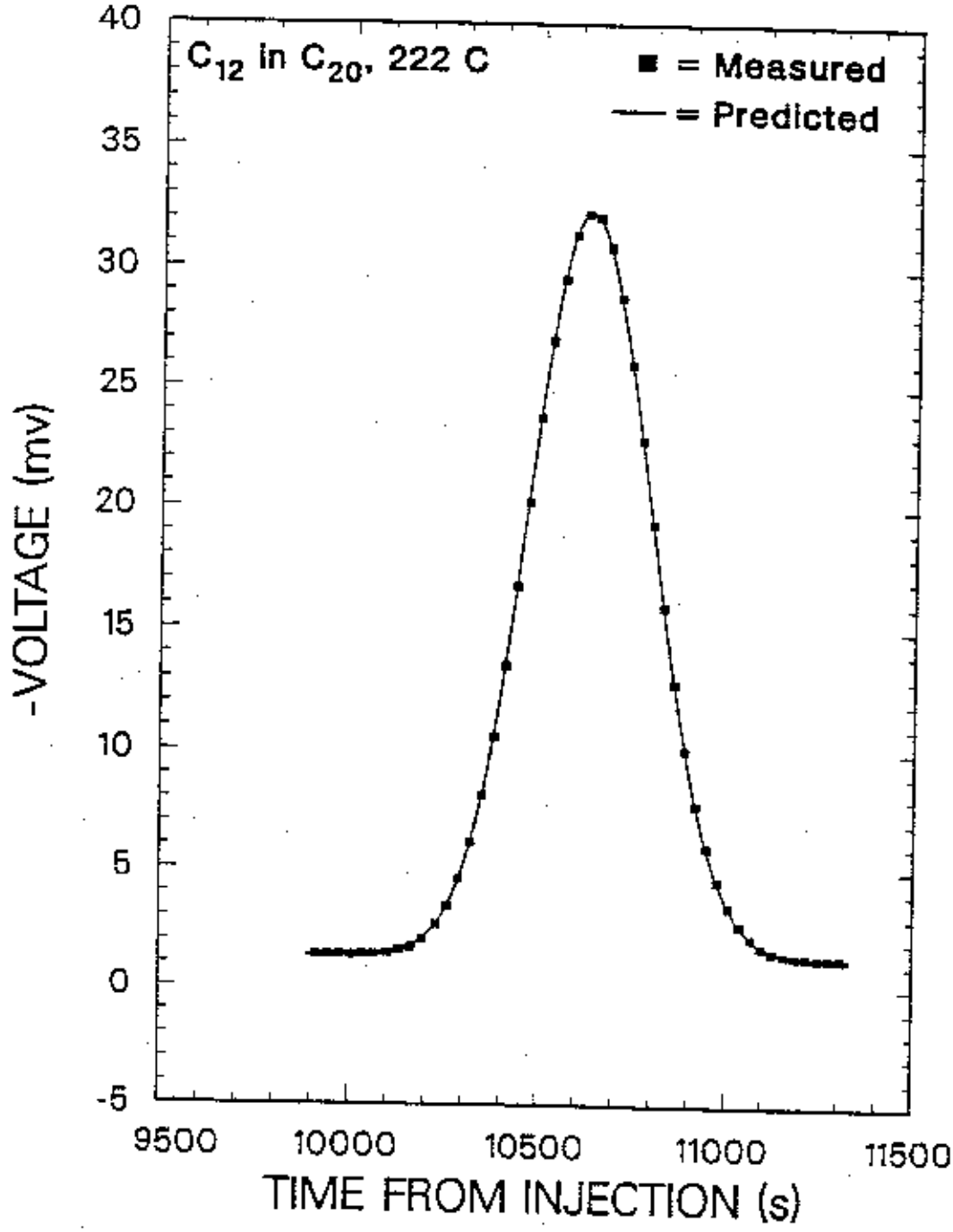

Figure 6.3. Model validation using a typical n-alkane solute peak.

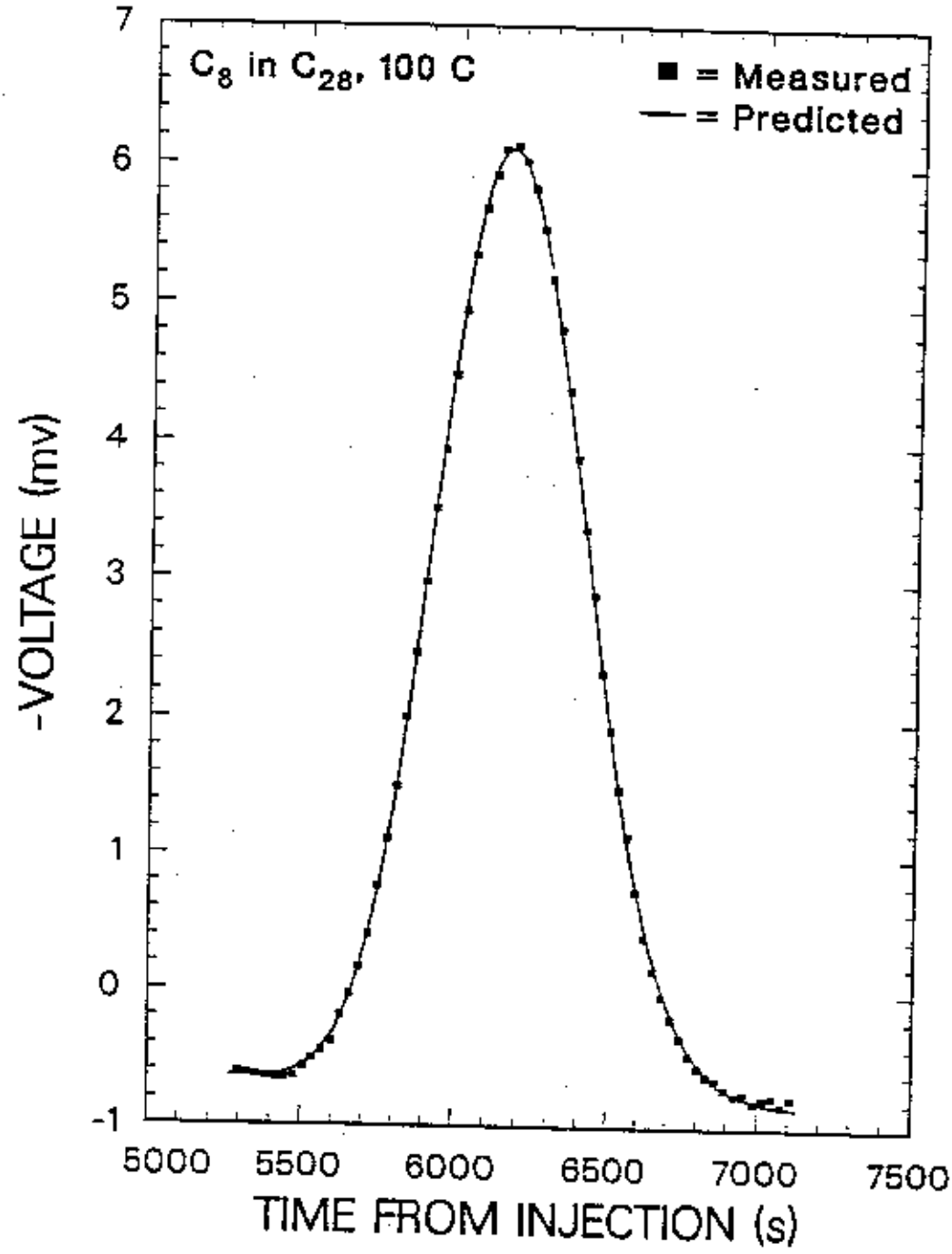

Figure 6.4. Model validation using a small n-alkane solute peak.

Table 6.1. Model Results for Fractional Peak Analysis
(n-Dodecane in n-Eicosane at 222°C, 200 psia)

x, percent of peak[1]	Number of data pts.	$D_{12} \times 10^9$ (m^2/sec)	Percent error
100[2]	287	4.630[3]	0.00[3]
95	160	4.629	−0.02
90	141	4.629	−0.02
85	128	4.629	−0.02
80	118	4.631	+0.02
60	90	4.633	+0.06
40	67	4.621	−0.20
20	45	4.587	−0.93
10	32	4.578	−1.12
5	23	4.550	−1.73
2	15	4.461	−3.65

1. See Equation (6.3).
2. Includes full peak with ample baseline on each side.
3. Full peak result assumed to be 'true' value.

level, the detectable limit was approximately 1 x 10^{-7} RIU. The manufacturer specified the noise level to be 4 x 10^{-8} RIU under the best possible operating conditions, which agreed closely with the experimental noise level of 5 x 10^{-8} RIU. This agreement indicated that the detector performed up to design specifications even at the 95°C detector cell temperature which was maintained to collected data using the solvent n-octacosane.

The effect of using only a portion of the peak was also investigated for the experimental peaks. The results of the fractional peak analyses for the example peaks are given in Appendix B and were typical of of the results for nearly all of the experimental peaks. The results for Example 2 are also shown in Table 6.1. The percentage of the peak, x, was defined by Equation 6.8. The percentage error was calculated by assuming that the diffusion coefficient for the full peak, including several minutes of baseline, was the true diffusion coefficient. The results

were startling. The diffusion coefficient was found to be nearly independent of the percentage of the peak used by the model until less than 40% of the peak was used in the calculations. These results proved that the new model was not significantly influenced by the selection of the peak end points. Even large portions of the peak tails could be eliminated from the analysis without significantly affecting the calculated diffusion coefficients.

E. SENSITIVITY ANALYSES

The measured values for the diffusion tube radius and length were given in Table 5.1. In this section the effect of uncertainty in these measurements upon the calculated diffusion coefficients was investigated. This potential source of error has been largely ignored in the literature.

Sensitivity analyses were performed using the non-linear least squares model for Taylor dispersion. Two previous example peaks from Section D were chosen for the analyses. The sensitivity analyses were performed by varying the nominal radius and the nominal length independently for each peak. The resulting diffusion coefficients were then calculated using the new peak analysis model.

The results of the radius sensitivity analysis for a carbon dioxide peak diffusing in n-eicosane are given in Table 6.2. Table 6.2 shows that the percent error in the diffusion coefficient is a linear function of the nominal radius. Recalling that the nominal measured radius was $(5.23 \pm 0.02) \times 10^{-4}$ m, the maximum potential error in the diffusion coefficient due to an error in the radius measurement was approximately 0.8% for this peak.

Table 6.3 gives the results of the length sensitivity analysis for the same peak. The model is almost unbelievably insensitive to length. In fact, even if a 10 m error

Table 6.2. Model Sensitivity to Measurement Uncertainty in the Dispersion Tube Radius[1]

(Carbon Dioxide in n-Eicosane, 222°C, 200 psia)

$a_o \times 10^4$ (m)	$a \times 10^4$ (m)	$D_{12} \times 10^9$ (m^2)	$\frac{D_{12}}{D_{12,\ rep.}}$	Percent Error
5.180	5.198	14.750	0.981	−1.91
5.190	5.208	14.808	0.985	−1.53
5.200	5.218	14.865	0.989	−1.15
5.210	5.228	14.922	0.992	−0.77
5.220	5.238	14.980	0.996	−0.38
5.230	5.248	15.037[2]	1.000	0.00
5.240	5.258	15.095	1.004	+0.38
5.250	5.268	15.153	1.008	+0.77
5.260	5.278	15.211	1.012	+1.15
5.270	5.288	15.269	1.015	+1.54
5.280	5.298	15.327	1.019	+1.93

1. a_o is the tube radius at 21°C and a is the corresponding temperature compensated radius actually used to calculate the diffusion coefficient.

2. $D_{12,\ rep.}$; the reported diffusion coefficient for this peak.

Table 6.3. Model Sensitivity to Measurement Uncertainty in the Dispersion Tube Length[1]

(Carbon Dioxide in n-Eicosane, 222°C, 200 psia)

L_o (m)	L (m)	$D_{12} \times 10^9$ (m^2)	$\frac{D_{12}}{D_{12,\ rep.}}$	Percent Error
33.55	33.67	15.062	1.002	+0.16
38.55	38.68	15.047	1.001	+0.07
43.55	43.70	15.037[2]	1.000	0.00
48.55	48.72	15.030	1.000	−0.05
53.55	53.74	15.025	0.999	−0.08

1. L_o is the length at 21°C and L is the corresponding temperature compensated length actually used to calculate the diffusion coefficient.

2. $D_{12,\ rep.}$; the reported diffusion coefficient for this peak.

had been made in the length measurement, the resulting diffusion coefficient would be in error by no more than 0.2%. However, it should be noted that the best fit parameters B_2 and B_4 change considerably as L is varied. When L is in error, B_2 is no longer related to the true Taylor dispersion coefficient, K, by a factor of four, and B_4 no longer represents the true solvent velocity. Still, the calculated diffusion coefficient is hardly affected by gross errors in L. As expected, the best fit parameters B_1, B_3, and B_5 remain unchanged as L is varied.

To confirm the results obtained with the carbon dioxide peak, the same sensitivity analyses were performed for a low temperature alkane peak. The results are presented in Tables 6.4 and 6.5. The results for the alkane solute peak sensitivity analyses agreed closely with the results for the gas peak. Again, the maximum error in the diffusion coefficient due to the uncertainty in the radius measurement was found to be 0.8%. The diffusion coefficient was insensitive to errors in the diffusion tube length measurement over a 20 meter range.

It can be concluded that while insensitive to errors in the measurement of diffusion tube length, the calculated diffusion coefficients are highly susceptible to relatively small errors in the tube radius measurement. The percentage error in the diffusion coefficient was found to be linear with radius and was estimated to be within $\pm 0.8\%$ for this study.

Table 6.4. Model Sensitivity to Measurement Uncertainty in the Dispersion Tube Radius[1]

(n-Octane in n-Octacosane, 100°C, 200 psia)

$a_o \times 10^4$ (m)	$a \times 10^4$ (m)	$D_{12} \times 10^9$ (m^2)	$\frac{D_{12}}{D_{12,\ rep.}}$	Percent Error
5.180	5.187	1.175	0.981	−1.90
5.190	5.197	1.179	0.985	−1.53
5.200	5.207	1.184	0.989	−1.14
5.210	5.217	1.189	0.992	−0.77
5.220	5.227	1.193	0.996	−0.38
5.230	5.237	1.198[2]	1.000	0.00
5.240	5.247	1.202	1.004	+0.38
5.250	5.257	1.207	1.008	+0.77
5.260	5.267	1.212	1.012	+1.15
5.270	5.277	1.216	1.015	+1.54
5.280	5.287	1.221	1.019	+1.92

1. a_o is the tube radius at 21°C and a is the corresponding temperature compensated radius actually used to calculate the diffusion coefficient.

2. $D_{12,\ rep.}$; the reported diffusion coefficient for this peak.

Table 6.5. Model Sensitivity to Measurement Uncertainty in the Dispersion Tube Length[1]

(n-Octane in n-Octacosane, 100°C, 200 psia)

L_o (m)	L (m)	$D_{12} \times 10^9$ (m^2)	$\frac{D_{12}}{D_{12,\ rep.}}$	Percent Error
33.55	33.59	1.198	1.000	0.00
38.55	38.60	1.198	1.000	0.00
43.55	43.61	1.198[2]	1.000	0.00
48.55	48.61	1.198	1.000	0.00
53.55	53.62	1.198	1.000	0.00

1. L_o is the length at 21°C and L is the corresponding temperature compensated length actually used to calculate the diffusion coefficient.

2. $D_{12,\ rep.}$; the reported diffusion coefficient for this peak.

F. COMPARISON TO OTHER ANALYSIS METHODS

Another important test of the model was to compare the model results to the results obtained using different analysis methods. Two cases were chosen for this purpose to illustrate the performance of the method for extremely different types of peaks. The first case consists of tall sharp peaks resulting from replicate gaseous injections at a relatively high temperature, while the second case consisted of short wide peaks resulting from replicate liquid alkane injections at a relatively low temperature.

Table 6.6 is a comparison of the resulting diffusion coefficients calculated for the first case using the moment method (Matthews, 1986), the computerized "graphical" method, and the method described in this chapter. The results shown in Table 6.6 were fairly typical for gaseous solute injections. The moment method yielded approximately the same average diffusion coefficient as the new model, but the standard deviation of the replicate injections was considerably larger. The computerized "graphical" method, which was included in the new model to determine an initial guess for D_{12}, yielded very reproducible results, but the average diffusion coefficient was nearly 6% less than the diffusion coefficient determined using the full dispersion model.

Table 6.7 gives the results for a fairly typical set of alkane peaks. Although the reproducibility of the three methods was similar, the average diffusion coefficient determined by the moment method was considerably higher than the average result determined by the other methods. The results of the computerized "graphical" method are in close agreement with the results of the full model developed during the work.

In general, the moment method agreed closely with the results of the new

Table 6.6. Results of Different Peak Analysis Methods for Replicate Gaseous Solute Peaks

(Carbon Dioxide in n-Eicosane at 222°C, 200 psia)
($10^9 D_{12}^o$, m^2/sec)

	Moment Method[1]	Graphical Method[2]	Non-Linear Curve Fit[3]
Peak #1	15.340	14.184	15.123
Peak #2	14.970	14.178	15.037
Peak #3	15.265	14.171	15.050
$\overline{D_{12}^o} \pm \sigma_{n-1}$	15.192 ± 0.196	14.178 ± 0.007	15.070 ± 0.046
% Error	+0.81	−5.92	NA[4]

Table 6.7. Results of Different Peak Analysis Methods for Replicate n-Alkane Solute Peaks

(n-Octane in n-Octacosane at 100°C, 200 psia)
($10^9 D_{12}^o$, m^2/sec)

	Moment Method[1]	Graphical Method[2]	Non-Linear Curve Fit[3]
Peak #1	1.432	1.241	1.231
Peak #2	1.396	1.222	1.229
Peak #3	1.418	1.182	1.198
$\overline{D_{12}^o} \pm \sigma_{n-1}$	1.415 ± 0.018	1.215 ± 0.030	1.219 ± 0.018
% Error	+16.1	−0.41	NA[4]

1. Results of method described by Matthews (1986).
2. Results of computer algorithm developed during this work which simulates the graphical method. The algorithm was used to generate initial guesses of D_{12}^o for the non-linear model.
3. Results of the full model developed during this work.
4. Non-linear curve fit result assumed to be 'true' D_{12}^o.

procedure only for tall, sharp, clean peaks which rose abruptly from the baseline. However, for wide peaks which gradually rose from the baseline, the moment method was often in error by several percent. These observed trends agree with the primary criticism of the moment method; the method heavily weights the tails where the uncertainty of the measurements is the greatest.

The general behavior of the computerized "graphical" method was opposite that of the moment method. The method worked best for short broad peaks, but failed for the sharp peaks which were indicative of gaseous solute injections. One possible reason for this behavior is that the method depends on the peak width at half height, which is much larger for wide peaks and therefore determined more accurately for such peaks. However, this reasoning does not explain the systematic low predictions of the diffusion coefficients which were observed for tall sharp peaks.

The reason why the "graphical" method fails miserably for tall, sharp peaks is more subtle. Cloeta et al. (1976) suggested that the half width may lead to systematic errors in the calculated variance for sharp peaks even when the half width is measured accurately.

Cloeta et al. (1976) presented a general equation relating the variance of the peak to the peak width at any fractional height $1/p$. Using this relationship, the parameter H, defined previously by Equation 2.8, can be written in general as;

$$H = \frac{LW_{1/p}^2}{(8 \log_e p) t_{max}^2} \tag{6.9}$$

Cloeta et al. (1976) did not give specific criteria for deciding which value of p to use for a particular peak. However, the authors warned that the half-height width is not necessarily the optimal measurement for estimating peak variance for all dispersion peaks. It was noted that the optimal value for p is actually a strong value of peak

shape and that further work to quantify the relationship between p and peak shape was necessary. Apparently the warning of Cloeta et al. (1976) has gone unheeded as researchers continue to rely solely on the half height width to calculate diffusion coefficients.

G. COMPARISON OF MODEL RESULTS TO LITERATURE VALUES

The final test of the model was to compare calculated diffusion coefficients to literature data where data was available. Unfortunately, diffusion coefficients have never been measured in n-eicosane or n-octacosane. However, a handful of data points from the previous study (Matthews, 1986) have been reported by others in the literature. Using the raw peak data from the previous study, the diffusion coefficients were calculated by the various methods. The results were then compared to the literature results in Table 6.8. Both the computerized "graphical" method and the full curve fitting procedure yielded results which were in close agreement with the literature. The largest disagreement for the new curve fitting method was only 2.8% (for hexadecane in heptane). The agreement was excellent considering the wide disparity of values for most liquid phase diffusion coefficient measurements which have been duplicated in the literature. The computerized "graphical" method performed equally well only because the peaks were wide. Unfortunately literature data corresponding to solute-solvent systems with larger diffusion coefficients (and therefore sharper peaks) were not available. If such data were available, the accuracy of the computerized "graphical" method would be expected to deteriorate as the magnitude of the diffusion coefficient increased.

As expected, the moment method did not predict the literature data nearly as well as the other methods since the comparisons were for wide alkane peaks. The

Table 6.8. Comparison of Calculated D_{12}° Results to Literature Values
(Solvent: n-Heptane at 25°C, 1 atm)
($10^9 D_{12}^{\circ}$, m^2/sec)

Solute	Moment Method[1]	Graphical Method[2]	Non-Linear Curve Fit[3]	Literature Values
n-octane	2.94	2.78	2.82	2.80[4]
n-dodecane	2.24	2.15	2.21	2.15[5]
n-tetradecane	2.05	1.92	1.92	1.89[5]
n-hexadecane	1.84	1.79	1.83	1.78[6]

1. Results of method described by Matthews (1986).
2. Results of computer algorithm developed during this work which simulates the graphical method. The algorithm was used to generate initial guesses of D_{12}° for the non-linear model.
3. Results of the full model developed during this work.
4. Alizadeh and Wakeham (1982). Technique: Taylor dispersion.
5. Lo (1974). Technique: Diaphragm cell.
6. Bidlack and Anderson (1964a). Technique: Optical diffusiometer.

largest deviation from the literature was 8.4% for the tetradecane data point. Both of the other analysis methods agreed and were within 1.6% of the literature value for this point. These results cast doubt on the accuracy of all previously reported measurements of diffusion coefficients calculated by finite summations of the peak moments.

H. SELECTION OF OPERATING FLOW RATE

The topic of solvent flow rate selection was included in this chapter because it is inherently linked to the mathematics of Taylor dispersion. In this section, several criteria which limit the operating solvent flow rate will be discussed.

1. Flow Criteria Based on Limitations of Taylor's Solution

Most recent Taylor dispersion experiments have been designed to meet the flow criterion given by Alizadeh and Wakeham (1982) and Alizadeh et al. (1980), which was based on the moment method solution. For this work, a new practical flow criterion was derived based on the analytical solution by Taylor (1953).

Obviously, as D_{12} approaches zero, Equation 2.5 does not reduce to the correct limit, since D_{12} appears in the denominator in the definition for K. The limitations of the solution were realized by Taylor (1953, 1954b) and later clarified by Hunt (1976). The solution given by Equation 2.5 is valid only when the following criterion is met (Hunt, 1976; and Taylor, 1953, 1954b);

$$\frac{D_{12}}{\overline{u}a} >> \frac{a}{4l_p} \tag{6.10}$$

where l_p was loosely defined as the length over which the gradient of $\partial C_a/\partial z$ is appreciable.

Assuming l_p to be the length occupied by the peak, it can be approximated by the product of average solvent velocity and peak width, W, which can be estimated from a chart recorder output tracing the detector signal. The inequality can then be written as;

$$W >> \frac{a^2}{4D_{12}} \tag{6.11}$$

Equation 6.11 can quickly be used to check the validity of the mathematical solution for D_{12} following an experiment. However, the form of the inequality does not allow it to be used in the design of an experiment since W, the peak width is not known apriori, and since $\overline{u}$ has been eliminated from the equation.

A method was derived for estimating the peak width apriori. Combining and

rearranging Equations 2.7 and 6.9 yields;

$$W_{1/p}^2 = \left(\frac{8 \log_e p}{\overline{u}^2}\right) \sigma_s^2 \tag{6.12}$$

Following Grushka and Kikta (1974), the spatial variance can be approximated by;

$$\sigma_s^2 = \frac{a^2 \overline{u} L}{24 D_{12}} \tag{6.13}$$

Combining Equations 6.12 and 6.13 gives an approximate expression for the peak width at any fractional height $1/p$.

$$W_{1/p} = a \left(\frac{L \log_e p}{3 \overline{u} D_{12}}\right)^{1/2} \tag{6.14}$$

Finally, substituting Equation 6.14 for the peak width into Equation 6.11 and rearranging terms gives a criterion for $\overline{u}$;

$$\overline{u} << \frac{16 \log_e p \; D_{12} L}{3a^2} \tag{6.15}$$

Recalling that the width term in Equation 6.14 represents the width of the full peak (the entire region where $\partial C_a / \partial z$ is appreciable), p was chosen conservatively to be 10, corresponding to a fractional peak height of 1/10. Actually $\partial C_a / \partial z$ is appreciable for much larger values of p, but using larger values would result in a more liberal flow criteria. Substituting $p = 10$ into Equation 6.15 gives the final operating criterion which ensures that the mathematical model is valid. The right hand side of Equation 6.15 was also divided by 10 to conservatively account for the double inequality. The final working criterion is then given by;

$$\overline{u} < \frac{D_{12} L}{a^2} \tag{6.16}$$

The form of this criterion agrees exactly with the form of the criterion given by Alizadeh and Wakeham (1982), even though their criteria was derived using a

completely different mathematical approach which applied to the moment method solution. However, the criteria of Alizadeh and Wakeham (1982) was a factor of 10 more stringent, indicating that Taylor's solution is less restricted than the moment solution given by Alizadeh et al. (1980). All of the experiments performed during this study safely met both the criterion given by Equation 6.16 and the more stringent criterion of Alizadeh and Wakeham (1982), verifying that the mathematical solution was valid for all of the experiments.

2. Laminar Flow Criterion

The solvent flow rate must also be slow enough so that laminar flow is maintained in the diffusion tube. However, this limitation is rarely a limiting criteria because the onset of turbulence does not occur until Reynolds numbers near 2000. The other flow criteria are more stringent and usually limit the Reynolds number for most solvents to well below 100. For this study the Reynolds number was always less than 15.

3. Coiling Effects

As mentioned in Chapter V, one of the greatest potential causes of error in a Taylor dispersion experiment is the effect of secondary flows in the diffusion tube due to the coiling of the tube. The true laminar flow profile is upset because fluid travelling near the outside of the coil travels a farther distance than fluid travelling near the inside of the coil. Unfortunately, coiling of the tube is necessitated in a practical apparatus, but it is possible to design and operate an apparatus so that the effect of coiling is minimized.

Golay (1979) and Nunge et al. (1972) have obtained approximate analytical solutions to the Taylor dispersion problem in a curved tube. Although the solution

of Nunge et al. (1972) was carried out to a higher order than Golay's (1979) solution, neither solution is accurate enough to use for actually determining the diffusion coefficient. Instead, the solutions are used to develop operating criteria for the experiment so that the effect of coiling does not appreciably affect the experimental results.

Golay (1979) defined a transition flowrate, Q_{TRANS}, as the volumetric flow rate in a curved tube where dispersion effects due to secondary flow become significant. The transition flowrate was given as;

$$Q_{trans} = (518aR_cD_{12}\eta/\rho)^{1/2} \tag{6.17}$$

where R_c is the radius of curvature for the diffusion coil.

Using the solutions of Golay (1979) and Nunge et al. (1972), Atwood and Golstein (1984) were able to demonstrate that both solutions could be approximated by the following form;

$$\frac{D_{12,obs}}{D_{12}} = \frac{1}{1-\alpha(Q/Q_{trans})^4} \tag{6.18}$$

where the constant $\alpha = 0.184$ for Golay's solution and $\alpha = 0.1034$ for Nunge's solution. D_{obs} is the apparent diffusion coefficient which would be observed of coiling were neglected in the mathematical analysis of diffusion. Figure 6.5 is a plot of Equation 6.18 for both solutions. The plot illustrates that if flowrate is not chosen carefully, highly erroneous values of the calculated diffusion coefficient will result.

Atwood and Goldstein (1984) performed Taylor dispersion experiments with several different solute-solvent systems and found that all of the data fell to the right of both curves in Figure 6.5, indicating that both criteria were too stringent, but that Nunge's criterion fit the data well for Q/Q_{TRANS} less than 1. Atwood

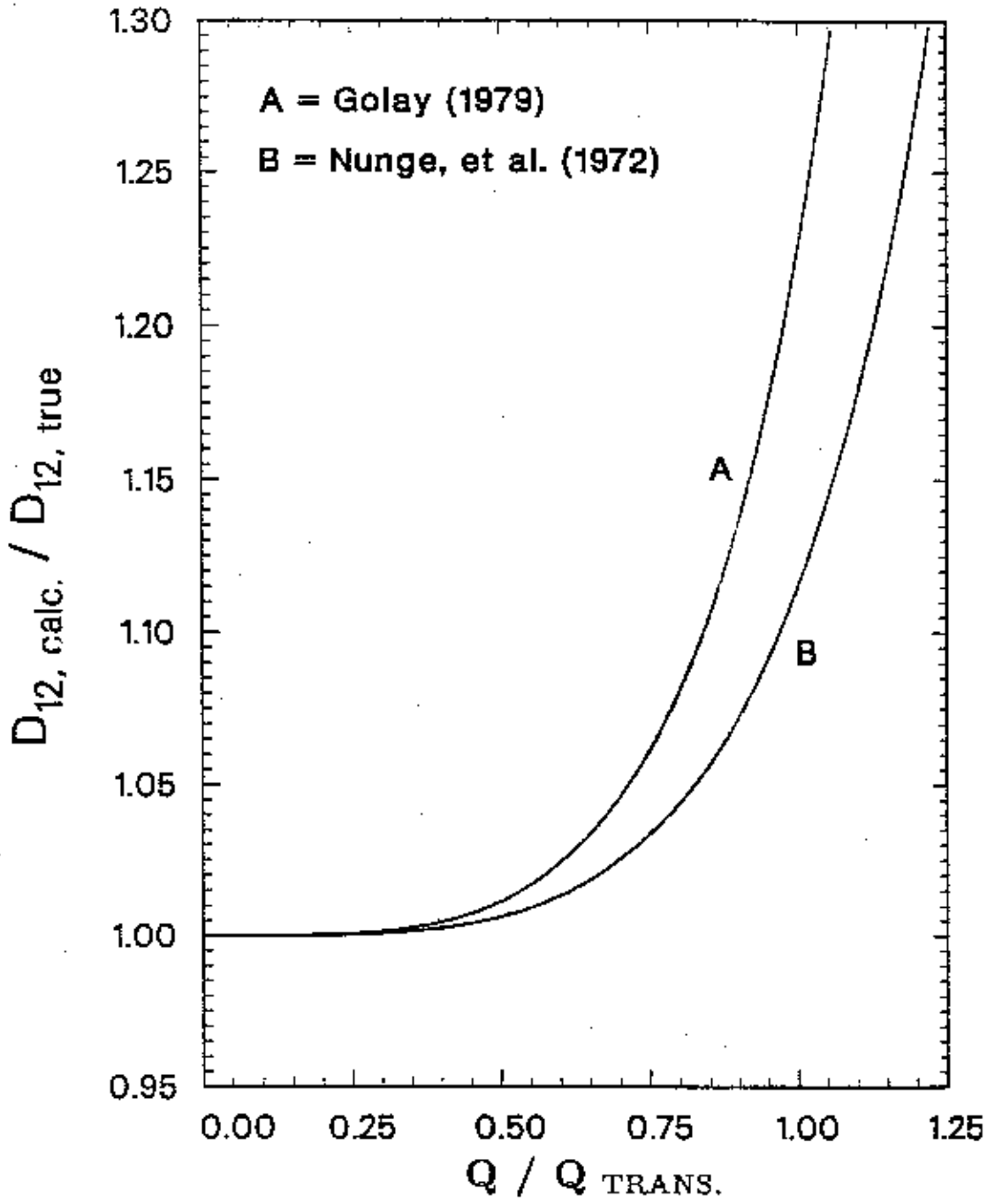

Figure 6.5. Effect of tube coiling on the calculated diffusion coefficients.

and Goldstein (1984) suggested that Nunge's solution be used as an upper bound for the effects of secondary flows.

Following the suggestion of Atwood and Goldstein (1984), Curve B from Figure 1 was used to estimate the maximum possible error due to coiling. Flowrates for the experiments ranged from 0.16 to 0.33 x 10^{-6} m^3/min (0.16 to 0.33 ml/min). For the experiments with n-eicosane, the flowrate was chosen so that the estimated error in the diffusion coefficient was minimal. For alkane solutes diffusing in n-eicosane, the estimated error ranged from +0.04 to +0.14%. For gaseous solutes in n-eicosane, the estimated error due to coiling was negligible, never exceeding +0.01%.

Throughout the experiments with the solvents n-octacosane and Fischer-Tropsch wax, the minimum operating flowrate of approximately 0.33 ml/min was determined by a physical limitation of the apparatus. The solvent delivery pump, which operated at temperatures in excess of 100°C, was unable to deliver a consistent continuous flow less than 0.33 ml/min under these extreme conditions. At this flowrate, the estimated maximum error due to coiling for the experiments with alkane solutes ranged from +0.3 to +1.6%. This error was a strong increasing function of solute carbon number and a weak increasing function of temperature. For gaseous solutes diffusing in n-octacosane and FT wax the estimated maximum error due to coiling was never greater than 0.1%.